Clinical and Experimental Medicine (2025) 25:88
https://doi.org/10.1007/s10238-025-01622-1

RESEARCH

MiR-101-3p targets the PI3K-AKT signaling pathway via Birc5 to inhibit invasion, proliferation, and epithelial–mesenchymal transition in hepatocellular carcinoma

Wenyuan Zhu[1] · Qingqiang Ni[1] · Zhengjian Wang[1] · Ruxuan Zhang[1] · Fangfeng Liu[1] · Hong Chang[1]

Received: 17 December 2024 / Accepted: 28 February 2025
© The Author(s) 2025

Abstract

MicroRNAs (miRNAs) are small non-coding RNA molecules that regulate numerous genes in cells. Abnormal expression of miRNAs can lead to cancer. However, the roles and underlying mechanisms of miRNAs in hepatocellular carcinoma (HCC) are not fully understood. Using molecular biology techniques, we designed eukaryotic expression vectors with enhanced expression of miR-101-3p to transfect human hepatocellular carcinoma cell lines. Subsequent to this, cell cloning experiments, CCK8 assays, and Transwell migration experiments were executed to assess their impact on liver cancer cell proliferation and invasion. Dual-luciferase assays were employed to validate the molecular interaction between miR-101-3p and Birc5. Through rescue experiments aimed at manipulating the expression levels of Birc5, we scrutinized the influence of miR-101-3p on liver cancer cell proliferation and invasion. Furthermore, Western blot analysis was utilized to monitor alterations in the expression levels of E-cadherin, N-cadherin, and vimentin proteins within each cell group. In vivo investigations were conducted using nude mice implanted with hepatocellular carcinoma cells transfected with Birc5. Additionally, further exploration was carried out by combining this model with the PI3K/AKT pathway inhibitor miltefosine to elucidate its effects on tumor proliferation. In vitro functional analysis of miR-101-3p revealed that treatment of HCC cells with its corresponding mimic significantly inhibited cell proliferation, colony formation, invasion, and epithelial–mesenchymal transition. Additionally, miR-101-3p exerts its anti-tumor effects by targeting the shared gene Birc5. Experiments using nude mouse models demonstrate that Birc5 promotes tumor proliferation by phosphorylating the PI3K/AKT signaling pathway. Inhibiting the PI3K/AKT signaling pathway shows suppressive effects on liver cancer proliferation. MiR-101-3p plays crucial roles in inhibiting the proliferation, invasion and epithelial–mesenchymal transition of HCC cells by targeting Birc5 and downregulating the PI3K-AKT signaling pathway. These findings provide new insights for the molecular treatment of HCC.

Keywords MiR-101-3p · Birc5 · Epithelial–mesenchymal transition · Invasion · Metastasis

Abbreviations

MiRNAs	MicroRNAs
HCC	Hepatocellular carcinoma
PLC	Primary liver cancer
EMT	Epithelial–mesenchymal transition
PI3K	The phosphoinositide 3-kinase
mTOR	Mammalian target of rapamycin
qRT-PCR	Real-time quantitative polymerase chain reaction
PBS	Phosphate-buffered saline
TBS	Tris-buffered saline
PVDF	Protein to polyvinylidene fluoride

Introduction

Primary liver cancer (PLC), commonly referred to as hepatocellular carcinoma (HCC), is a globally common malignant tumor of the digestive system. Its annual incidence is 841,000 cases worldwide (sixth among all malignancies) and annual mortality is 782,000 deaths (second among all malignancies) [1, 2]. It is particularly common in China, ranking

Joint first authors: Wenyuan Zhu and Qingqiang Ni

✉ Fangfeng Liu
liufangfeng@sdfmu.edu.cn

✉ Hong Chang
changhong@sdfmu.edu.cn

[1] Department of Hepatobiliary Surgery, Shandong Provincial Hospital, Shandong University, Jinan 250021, Shandong, China

Published online: 19 March 2025

fourth among common malignant tumors and second among tumor-related causes of death. The high mortality of HCC is closely associated with its recurrence, metastasis, epithelial–mesenchymal transition (EMT), and malignant proliferation, which are crucial mechanisms initiating and promoting tumor invasion and metastasis [3]. In EMT, epithelial cells affected by certain physiological or pathological factors lose cell polarity, break intercellular tight junctions and adhesion connections, and transform into cells with mesenchymal morphology and characteristics, thereby acquiring invasive and migratory capabilities [4, 5]. Recent research has shown that EMT plays a crucial role in the invasion and metastasis of HCC [6, 7]. In HCC, EMT and malignant proliferation are influenced by the activation of oncogenes, inactivation of tumor suppressor genes, and changes in miRNA expression profiles, leading to signaling pathway alterations such as activation of the phosphoinositide 3-kinase (PI3K)/AKT/mammalian target of rapamycin (mTOR), rat sarcoma/Raf/MEK/extracellular signal-regulated kinase, and vascular endothelial growth factor/vascular endothelial growth factor receptor pathways. These changes induce malignant transformation, inhibit cell apoptosis, and enhance proliferation and migratory capabilities, thereby altering the biological activity of tumor cells [8–10].

MiRNAs exhibit abnormal expression in various tumors, participating in tumor occurrence and development by regulating processes such as cell proliferation, migration, invasion, and apoptosis. They hold potential applications in early diagnosis, prognostication, prevention, and treatment of tumors. Numerous studies have demonstrated that genetic alterations (including genetic and epigenetic changes) in various cancers lead to abnormal miRNA expression, causing dysregulation of target gene expression. Therefore, miRNAs are closely associated with tumor pathogenesis, including cell proliferation, survival, and invasion [11]. Recent studies have shown that miRNA-101 plays a crucial regulatory role in the occurrence and development of diseases such as liver fibrosis, cardiovascular diseases, and cancer, making it a focus of cancer research [12, 13]. Other studies have revealed that miR-101 inhibits cell proliferation in various tumors [14–17] and upregulates E-cadherin expression, thereby inhibiting EMT. Furthermore, miR-101-3p, an important mature form of miR-101, plays an important role in the pathogenesis of various tumors because it is associated with tumor development and progression. Increased miR-101-3p expression inhibits the migration of ovarian cancer cells [18]. The miR-101-3p level is also reduced in glioblastoma stem cells; its overexpression leads to decreased cell proliferation, migration, and invasion [19]. Wang et al. [20] found that miR-101-3p promotes apoptosis in oral cancer cells by targeting BICC1.

Birc5, a member of the inhibitor of apoptosis protein gene family, regulates the physiological development and cell cycle of embryonic cells. It has dual effects of inhibiting apoptosis and promoting cell proliferation. Birc5 overexpression inhibits apoptosis through various mechanisms, leading to abnormal cell proliferation [21–24], and is closely associated with the malignant biological behavior of tumors. During HCC development, a high level of Birc5 induces tumor stromal angiogenesis and reduces cancer cell sensitivity to radiotherapy and chemotherapy, influencing the prognosis of HCC patients [25]. Birc5 exhibits highly selective positive expression in malignant tumors; its expression is related to high proliferative activity, recurrence potential, metastatic ability, resistance of tumors to radiotherapy and chemotherapy, and poor prognosis among patients with malignant tumors [26].

We investigated the expression of miR-101-3p and Birc5 in human HCC cell lines and HCC tissues. Furthermore, we explored the functional role of miR-101-3p in HCC cells. In HCC cell lines and tissues, the expression levels of miR-101-3p and Birc5 were negatively correlated. Additionally, luciferase reporter gene assays confirmed the targeted binding of miR-101-3p to Birc5. Finally, the interaction between miR-101-3p and Birc5 was confirmed using real-time quantitative polymerase chain reaction (qRT-PCR), Western blotting, and luciferase assays. Our results reveal novel molecular mechanisms involved in HCC progression and provide new treatment targets for HCC.

Materials and methods

Antibodies and reagents

Akt (1:1,000; proteintech. 10,176–2-AP), p-Akt (1:1,000; proteintech. 66,444–1-Ig) and PI3k (1:1,000; proteintech. 20,584–1-AP) were obtained from Proteintech Group, Inc (Wuhan, China). p-PI3k (1:1,000; Cell Signaling. 20,584–1-AP) was obtained from Cell Signaling Technology, Inc. (Danvers, MA, USA). Vimentin (1:1,000; HUABIO,ET1610-39), E-cadherin (1:1,000; HUABIO,EM0502) and N-cadherin (1:1,000; HUABIO,ET1607-37) were obtained from HUABIO (HangZhou, China). Monoclonal rabbit antibodies against Birc5 (1:2,000; Zhongshan Golden Bridge, ZB-2301), Anti-Mouse Secondary Antibodies (1:2,000; Zhongshan Golden Bridge. ZB-2305) and actin (1:1,000; Zhongshan Golden Bridge. TA-09) were purchased from Beijing Zhongshan Golden Bridge Biotechnology Co. Ltd.(China).

Cells and tissues

The cell lines used in this study were obtained from Cellverse Bioscience Technology Co., Ltd. (Shanghai, China). HCC tissues and adjacent non-cancerous tissues were obtained

from four patients with HCC who had been diagnosed at the Shandong Provincial Hospital. Specimens were preserved in liquid nitrogen, and all patients provided informed consent for analysis of their tissues. The study protocol was approved by the Ethics Committee of Shandong Provincial Hospital (approval no. SWYX:NO.2022–477).

Cell culture

HepG2 and Huh7 cells were cultured in DMEM (MACGENE, Beijing, China) medium, whereas L02, MHCC97L, and QGY7701 cells were cultured in 1640 (MACGENE, Beijing, China) medium. When cells reached 80–90% confluence in the culture dish, the cells were passaged, placed in a − 80 °C freezer overnight, transferred to cryogenic vials, and stored in liquid nitrogen.

Cell transfection

Cell transfection was performed in several steps. First, cells were allowed to reach the logarithmic growth phase, digested with trypsin, centrifuged, suspended, and seeded in six-well plates at 80% confluence. Second, 100 nM miRNA was thoroughly mixed in 150 μL of serum-free Opti-MEM I Reduced Serum Medium and incubated at room temperature for 5 min (Solution A). Third, an appropriate quantity of Lipofectamine 2000 was dissolved in 150 μL of serum-free Opti-MEM I Reduced Serum Medium and incubated at room temperature for 5 min (Solution B). Fourth, the two solutions were mixed at a ratio of 1:1 to achieve a total volume of 300 μL, then incubated at room temperature for 15 min. Fifth, 250 μL of the complex and 1 mL of serum-free Opti-MEM I Reduced Serum Medium were added to each well of a six-well plate and mixed thoroughly in a criss-cross pattern. Sixth, the cells were cultured at 37 °C in a CO_2 incubator for 4–6 h, and the medium was replaced. Finally, the samples were collected 24 h after transfection for further experiments.

qRT-PCR analysis

Total RNA was extracted using FastQuant cDNA First Strand Synthesis Kit (Genome Eraser) (KR116), in accordance with the manufacturer's instructions. A 1.0% agarose gel was prepared, and a nucleic acid dye was used for staining during agarose gel electrophoresis at a voltage of 18 V/cm for 20 min. Images were captured using a UV gel imaging system. After thorough mixing, real-time qRT-PCR was performed for RNA detection; amplification conditions were 95 °C for 15 min, followed by 40 cycles of 95 °C for 10 s and 60 °C for 30 s. Each sample was analyzed three times, and experimental data were analyzed using the $2^{-\Delta\Delta}$ CT method. The following primer sequences were used: hsa-miR-101-3p-RT: GTCGTATCCAGTGCAGGGTCCGAGGTATTCGCACTGGATACGACTTCAGT; hsa-miR-101-3p-F: GCGCGCGTACAGTACTGTGATA; hsa-miR-101-3p-R: AGTGCAGGGTCCGAGGTATT; Birc5-F: ACGACCCCATGCAAAGGAAA; and Birc5-R: ACAGCATCGAGCCAAGTCAT.

CCK-8 assay

Cells in the logarithmic growth phase were digested with trypsin and suspended at a concentration of $1–10 \times 10^4$ cells/mL. Approximately 5×10^3 cells were seeded in each well of a 96-well plate, with 100 μL of cell suspension per well. The culture plate was pre-incubated at 37 °C and 5% CO_2 for 24 h. Subsequently, the culture medium was replaced with 200 μL of media containing drugs with different concentrations among cells, whereas the control group was replaced with medium containing the solvent. Each sample concentration had five replicates. The culture plate was incubated for an appropriate duration. Then, 10 μL of CCK-8 solution were added to each well. The culture plate was incubated for an additional 1–4 h. Absorbance was measured at 450 nm using a microplate reader.

Transwell migration assay

After cell digestion, a single-cell suspension was prepared by resuspending cells in the culture medium. After cells had been counted, the cell concentration was adjusted to 2.5×10^5 cells/mL. Transwell migration chambers were assembled in a 24-well plate; 500 μL of culture medium containing 10% fetal bovine serum were added to the lower chamber, and 300 μL of cell-containing, serum-free medium were added to the upper chamber. Plates containing the Transwell chambers were incubated at 37 °C for 24 h, then rinsed with phosphate-buffered saline (PBS). Next, cells were fixed with 4% paraformaldehyde solution for 30 min and rinsed with PBS three times. After cells had been mixed with 0.1% crystal violet staining solution for 10 min, they were rinsed with running water. Non-migratory cells in the upper layer were gently removed with a cotton swab. The remaining cells were allowed to dry naturally. A fluorescence microscope was used to observe the cells and capture images. Two fields were randomly selected for each specimen (100 × and 200 ×), and the mean value was recorded.

Western blotting analysis

For Western blotting analysis, cells were washed three times with PBS. Then, they were mixed with 100 μL of 1 × SDS-PAGE protein (Beyotime Biotechnology, China) loading buffer and scraped. The scraped cells were incubated in a 100 °C metal bath for 10 min to facilitate protein

denaturation. Next, a polyacrylamide gel was prepared by combining the SDS-PAGE electrophoresis buffer, transfer buffer, and Tris-buffered saline (TBS) buffer (Meilunbio, China). Electrophoresis was performed at 80 V. When bromophenol blue in the sample reached the separation gel, the voltage was increased to 120 V. A standard wet transfer apparatus was used to transfer the designated target protein to polyvinylidene fluoride (PVDF) membrane. The primary antibody was diluted using Western blotting antibody dilution (1:1000,Servicebio, China) buffer and incubated with the membrane at 4 °C overnight; the membrane was then washed three times (10 min each) with 1 × TBST (TBS plus Tween). Subsequently, the secondary antibody was diluted in Western blotting antibody dilution (1:2000,Servicebio, China) buffer and incubated with the membrane at room temperature on a shaker for 1 h. After incubation, the membrane was washed three times with 1 × TBST for 10 min per wash. Finally, the PVDF membrane was placed in a chemiluminescence instrument and a 1:1 mixture of exposure solutions A and B was evenly applied.

Dual-luciferase assay

For the dual-luciferase assay, Birc5 3′-UTR fragments, including both wild-type and mutant, were synthesized and cloned into the pmirGLO vector. Subsequently, miR-101-3p and/or Birc5 3′-UTR were transfected into 293 T cells. After transfection, the cell culture medium was discarded, and the cells were washed twice with PBS. Then, 20 μL of 1 × Cell Lysis Buffer were added to each well and incubation at room temperature was performed for 5 min. The cell lysate was pipetted up and down to ensure thorough mixing before transfer to a 1.5-mL centrifuge tube. The tube was centrifuged at 12,000 g at room temperature for 2 min, and the supernatant was collected for subsequent analysis. The enzyme plate was prepared by adding 100 μL of Luciferase Substrate at room temperature. Next, 20 μL of cell lysate was pipetted into each well of the enzyme plate and mixed rapidly. Firefly luciferase reporter gene activity was immediately detected using a multifunctional microplate reader. Next, 100 μL of freshly prepared Renilla substrate working solution were added to the reaction solution and mixed rapidly. Renilla luciferase reporter gene activity was immediately detected using a microplate reader. A dual-luciferase reporter vector was constructed by synthesizing wild-type (3′UTRwt) and mutant (3′UTRmut) Birc5 3′-UTR fragments, then cloning them into the pmirGLO vector. After the pmirGLO dual-luciferase plasmid had been transfected into the cells, mRNA comprising the luc2 + Birc5 3′-UTR region was transcribed. If miR-101-3p bound to the mRNA containing Birc5 3′-UTR in a complementary manner, the expression activity of the luc2 luciferase was significantly affected. The regulatory effect of miR-101-3p on Birc5 mRNA was quantified by detecting the fluorescence intensity of the luc2 luciferase [27–29].

Transfection of miR-101-3p and Birc5-specific siRNA

HepG2 cells were seeded into 6-well plates at a density of 5×10^5 cells per well and incubated at 37 °C in a CO_2 incubator until 60–80%confluence was reached. Transfection of miR-101-3p and Birc5-specific siRNA was performed using Lipofectamine 2000(Invitrogen) according to the manufacturer's instructions. Briefly, cells were transfected with miR-101-3p and Birc5-specific siRNA in Opti-MEM medium. After 6 h of incubation, the medium was replaced with fresh DMEM containing 10%fetal bovine serum(FBS). Cells were further cultured for 72 h before being collected for subsequent experiments.

Nude mouse xenograft formation

Fifteen male BALB/c nude mice, aged 4–6 weeks and weighing 18–22 g, were purchased from the Experimental Animal Center of Shandong University. After 1 week of adaptation feeding, each mouse was randomly allocated to one of three groups: control, OV, and OV + pathway inhibitor (five mice/group). Cells in the logarithmic growth phase from each group were prepared in suspension at a concentration of 5×10^7 cells/mL. Subsequently, the cell suspensions were mixed with the gel matrix at a 1:1 ratio, and 0.2 mL were subcutaneously inoculated into the axillary region of each nude mouse (1×10^7 cells/mouse) to establish a nude mouse xenograft model. When tumors appeared, calipers were used to measure the long and short diameters of each tumor. Tumor volume (V) was calculated as $(\text{length} \times \text{width}^2)/2$, and the mean tumor volumes for each group were used to construct growth curves. After completion of the experiment, the tumors were meticulously dissected; tumor masses and volumes were calculated.

Immunohistochemistry

Fresh tissues were fixed in 4% paraformaldehyde; experimental sections were labeled and incubated in an oven at 60 °C for 2 h. Subsequently, the sections were immersed in a solution of 3% hydrogen peroxide; this was followed by the dropwise addition of blocking solution. Primary antibodies diluted in PBS were added dropwise onto the sections. The sections were horizontally oriented in a humid chamber and incubated overnight at 4 °C. Afterward, the slides were washed three times with PBS (pH 7.4) on a decolorization shaker for 5 min per wash. After sections had slightly dried, the corresponding species-specific secondary antibody (CY3-labeled GB210303; Servicebio, Wuhan, China) was applied to each section within the circular area and covered

for incubation at room temperature for 50 min in the dark. Freshly prepared DAB color solution (PA140212; Tiangen, Beijing, China) was used to develop color within the circular area during monitoring under a microscope. Harris hematoxylin (BOSTER AR1108) was utilized as a nuclear counterstain, and positive staining exhibited brown-yellow appearance.

Statistical analysis

Experimental data were analyzed using GraphPad Prism (version 8.0; GraphPad Software Inc., San Diego, CA, USA). The results are presented as the means ± standard deviations of three independent experiments. Statistical analysis was conducted using one-way analysis of variance, followed by Dunnett's t test. *P*-values < 0.05 were considered statistically significant.

Results

Expression and biological function of miR-101-3p in HCC cells

miRNAs are closely associated with tumor occurrence and development [11] and they play crucial roles in the biological processes of HCC cells. To explore miRNAs influencing the biological functions of HCC cells, we analyzed the differential expression of miRNAs between HCC and normal tissues using the TCGA database. We identified miR-101-3p as a differentially expressed miRNA, with lower expression in HCC tissues than in normal tissues (Fig. 1A). The downregulation of miR-101-3p was associated with a poor prognosis in HCC patients (Fig. 1B). Furthermore, we examined the expression levels of miR-101-3p in clinical samples and cell lines, revealing significantly lower expression in HCC cell lines such as QGY7701 and HepG2 than in normal cells (Fig. 1C). Therefore, we hypothesized that reduced miR-101-3p expression was linked to malignant behavior in HCC cells.

In this study, we used a miRNA mimic negative control whose sequence was designed based on cel-mir-239b to ensure no homology to the mammalian gene. To exclude nonspecific transfection effects and to serve as a baseline for evaluating miRNA mimic effects. We investigated the biological role of miR-101-3p in the growth of HCC cells through in vitro experiments. Two HCC cell lines, OGY7701 and HepG2, were selected for these experiments. CCK-8 assays showed that miR-101-3p overexpression significantly inhibited the proliferation of OGY7701 and HepG2 cells (n = 3, $p < 0.05$, Fig. 1D). Colony formation experiments demonstrated that miR-101-3p overexpression significantly suppressed the growth of OGY7701 and HepG2 cells (n = 3, $p < 0.05$, Fig. 1E). Transwell cell invasion assays revealed that the number of cells penetrating the polycarbonate membrane was significantly lower in the miR-101-3p overexpression group, indicating that miR-101-3p expression inhibits the invasive ability of HCC cells (n = 3, $p < 0.05$, Fig. 1F). Conversely, when the expression of miR-101-3p was inhibited, the invasive ability of HCC cells was enhanced. Therefore, we hypothesized that miR-101-3p plays crucial roles in HCC invasion and metastasis.

To validate this hypothesis, we performed Western blotting experiments, which showed significant increases in E-cadherin, an epithelial marker, at the protein levels in the miR-101-3p overexpression group. Conversely, the expression levels of vimentin and N-cadherin, components associated with the mesenchymal phenotype, were both reduced at the protein levels (n = 3, $*p < 0.05$, Fig. 1G). These findings suggest that miR-101-3p inhibits the invasive ability of HCC cells by preventing EMT. Overall, the results indicate that miR-101-3p overexpression can inhibit malignant behavior in HCC cells.

Associations of Birc5 expression with proliferation and invasion abilities of HCC cells

For elucidation of the anti-tumor role of miR-101-3p in HCC, we used TargetScan software to identify potential targets of miR-101-3p; we found a binding site in Birc5. Previous studies have found that Birc5 is overexpressed in a variety of cancers, and its high expression is closely related to poor prognosis of patients [30]. Birc5 (survivin) has also been shown to induce EMT in HCC cells [31]. Therefore, Birc5 was selected as the target gene in this study. Assistant for Clinical Bioinformatics analysis confirmed that Birc5 expression was significantly higher in HCC tissues than in normal tissues (Fig. 2A); expression was higher in HCC stages III and IV than in stages I and II (Fig. 2B). Kaplan–Meier survival analysis revealed a worse prognosis for patients with high Birc5 expression than for patients with low expression (Fig. 2C). Furthermore, protein immunoblotting on four pairs of HCC tissues and matched adjacent tissues demonstrated higher Birc5 expression in HCC tissues ($p < 0.05$, Fig. 2D). Subsequently, we conducted transfection experiments on OGY7701 and HepG2 HCC cell lines to construct a Birc5 overexpression cell group and a negative control cell group. Cell cloning and CCK-8 assays demonstrated significantly higher proliferation rates in the Birc5 overexpression group than in the negative control group (n = 3, $p < 0.05$, Fig. 2E, F). Furthermore, Transwell migration assays indicated a significant increase in the invasive ability of HCC cells with Birc5 overexpression, suggesting an association between Birc5 overexpression and enhanced proliferation and invasion abilities in HCC cells (n = 3, $p < 0.05$, Fig. 2G).

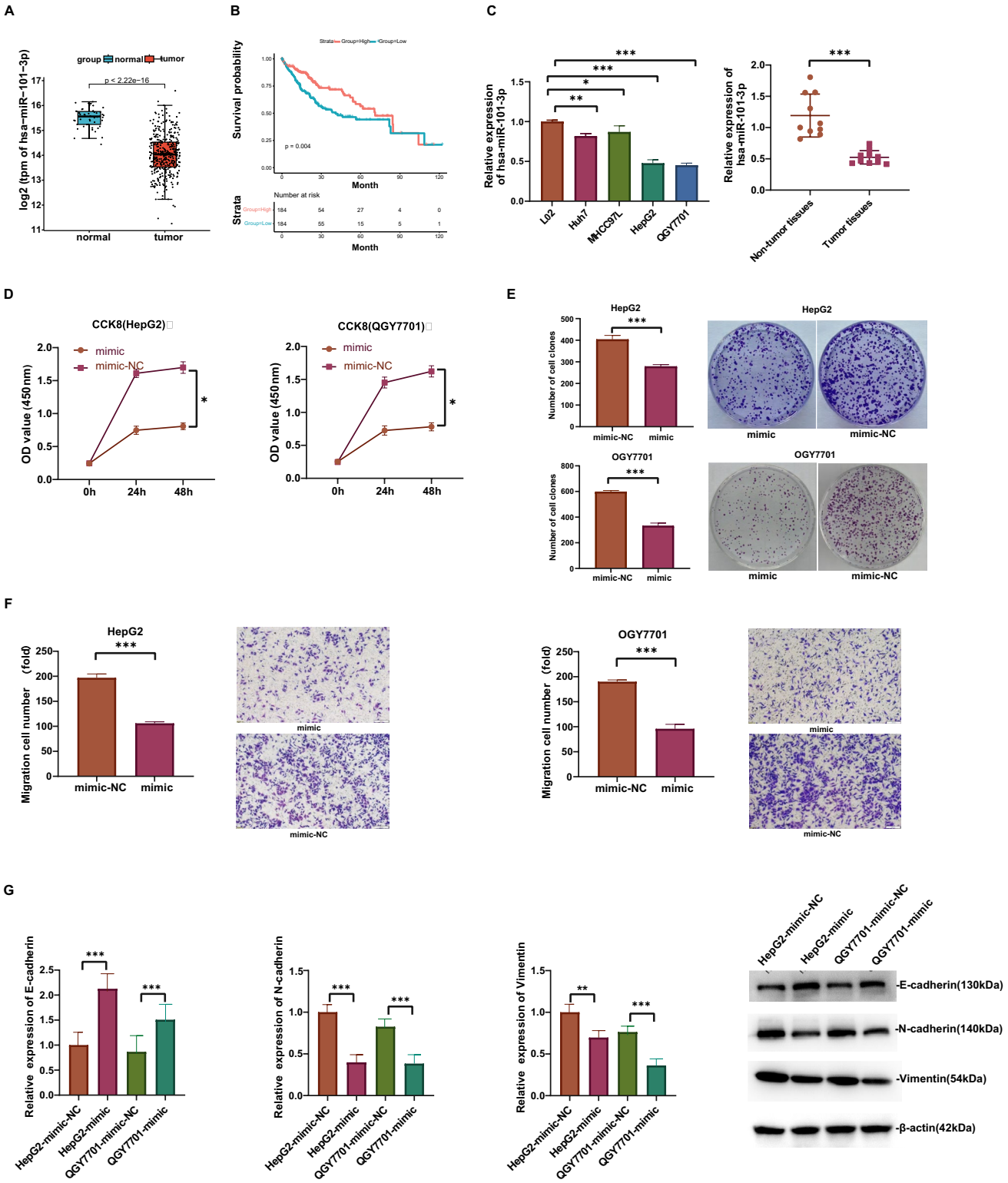

In protein immunoblotting experiments, we compared the protein expression levels of EMT-related genes between the Birc5 overexpression group (ov) and the negative control group (ov-NC) (Fig. 2H). The Birc5 overexpression group showed significant decreases in E-cadherin expression at protein levels, whereas the expression levels of mesenchymal markers (e.g., vimentin and N-cadherin) were elevated, indicating that Birc5 promotes EMT in HCC cells. qRT-PCR analysis showed that miR-101-3p overexpression suppressed Birc5 expression in HCC tissues (n = 3, $p < 0.05$, Fig. 2I),

◂**Fig. 1** High miR-101-3p expression inhibits proliferation and invasion in HCC cells. **A** miR-101-3p expression levels were significantly higher in normal tissues than in HCC tissues. **B** Low miR-101-3p expression was associated with poor patient prognosis. **C** qRT-PCR was used to measure the expression levels of miR-101-3p in normal cell lines, HCC cell lines, HCC tissues, and normal tissues. The results demonstrate that miR-101-3p expression is lower in HCC cells and tissues compared to normal cells and tissues. **D** mimic-NC was the negative control group, and mimic was the experimental group with miR-101-3p overexpression. CCK-8 assay analyzing cell proliferation. **E** Colony formation assay was conducted to compare the proliferative capacity of HCC cells between the two groups. **F** Transwell assay analyzing invasion capacity in HCC cells. **G** WB analysis was performed to compare the expression levels of E-cadherin, N-cadherin, and Vimentin proteins in HCC cells between the two groups

suggesting that miR-101-3p exerts anti-tumor effects by targeting Birc5.

MiR-101-3p exerts anti-tumor effects by targeting Birc5

Based on our finding that miR-101-3p may exert its effects by targeting Birc5, we performed transfection experiments to overexpress the *Birc5* gene using miR-101-3p overexpression and underexpression. qRT-PCR and Western blot analysis indicated that the mRNA and protein expression levels of Birc5 gene in the Birc5 overexpression group (ov) were significantly higher than those in the Birc5 negative control group (ov-NC) (n = 3, $p < 0.05$, Fig. 3A). To determine whether Birc5 displays miR-101-3p-responsive elements in its 3′ untranslated region (3′UTR), we synthesized a Birc5 3′-UTR fragment (wild-type + mutant) and cloned it into the pmirGLO vector, yielding a dual-luciferase reporter vector that contained the wild-type 3′UTR (3′UTRwt) and mutant-type 3′UTR (3′UTRmut). We found that miR-101-3p reduced the luciferase activity of the 3′UTRwt but not the 3′UTRmut (n = 3, $p < 0.05$, Fig. 3B), suggesting that Birc5 is a direct functional target of miR-101-3p and that miR-101-3p can bind to the Birc5 3′-UTR site to inhibit Birc5 expression, exerting its anticancer effects. To further validate that the target gene of miR-101-3p is Birc5, we performed knockdown experiments and detected the mRNA expression levels of miR-101-3p and Birc5 in cells of each group using qRT-PCR. The results (Fig. 3C) showed that in the cell group transfected with miR-101-3p-specific siRNA, the expression level of miR-101-3p was significantly decreased (n = 3, $p < 0.05$), while the mRNA expression level of the Birc5 gene was significantly higher than that in the control group (n = 3, $p < 0.05$). In the miR-101-3p overexpression group, the mRNA expression level of the Birc5 gene was significantly lower than that in the control group (n = 3, $p < 0.05$). In the cell group transfected with Birc5-specific siRNA, the mRNA expression level of the Birc5 gene was significantly lower than that in the control group (n = 3, $p < 0.05$), whereas there was no significant change in the expression level of miR-101-3p. In the cell group co-transfected with miR-101-3p and Birc5-specific siRNAs, the expression level of miR-101-3p was significantly decreased (n = 3, $p < 0.05$), while the expression level of Birc5 showed no significant change (n = 3, $p > 0.05$). In the Western blot analysis (Fig. 3D), the protein expression level of the Birc5 gene in the cell group transfected with miR-101-3p-specific siRNA was significantly higher than that in the control group (n = 3, $p < 0.05$). In the miR-101-3p overexpression group, the protein expression level of the Birc5 gene was significantly lower than that in the control group (n = 3, $p < 0.05$). In the cell group transfected with Birc5-specific siRNA, the protein expression level of the Birc5 gene was significantly lower than that in the control group (n = 3, $p < 0.05$). In the cell group co-transfected with miR-101-3p and Birc5-specific siRNAs, there was no significant difference in the protein expression level of the Birc5 gene compared with the control group (n = 3, $p > 0.05$). These findings suggest that miR-101-3p can negatively regulate the expression of the Birc5 gene.

Next, we transfected the Birc5 expression vector into miR-101-3p-overexpression OGY7701 and HepG2 cells. CCK-8 assays demonstrated that Birc5 overexpression attenuated the inhibitory effect of miR-101-3p overexpression on the proliferation of HCC cells (n = 3, $p < 0.05$, Fig. 3E). Colony formation assays also showed that Birc5 overexpression partially attenuated the growth inhibition induced by miR-101-3p expression in OGY7701 and HepG2 cells (n = 3, $p < 0.05$, Fig. 3F). Transwell assays (Fig. 3G) revealed that Birc5 overexpression attenuated the inhibitory effect of miR-101-3p on the invasive ability of HCC cells, leading to enhanced invasion. We investigated the impact of Birc5 overexpression on EMT in HCC cells through protein immunoblotting (n = 3, $p < 0.05$, Fig. 3H). The results showed that the protein expression levels of N-cadherin and vimentin were significantly higher in the HepG2 mimic + ov group (overexpressing both miR-101-3p and Birc5) than in the HepG2 mimic + ov-NC group (overexpressing only miR-101-3p), whereas E-cadherin expression was lower in the HepG2 mimic + ov group than in the HepG2 mimic + ov-NC group. Similarly, in the QGY7701 mimic + ov group, the expression levels of N-cadherin and vimentin were significantly higher, and E-cadherin expression was lower, than levels in the QGY7701 mimic + ov-NC group. These findings suggest that *Birc5* overexpression reverses the effect of miR-101-3p, promoting EMT in HCC cells. When miR-101-3p interferes with the *Birc5* target gene, E-cadherin expression increases, indicating that miR-101-3p targets Birc5 to inhibit EMT in HCC cells.

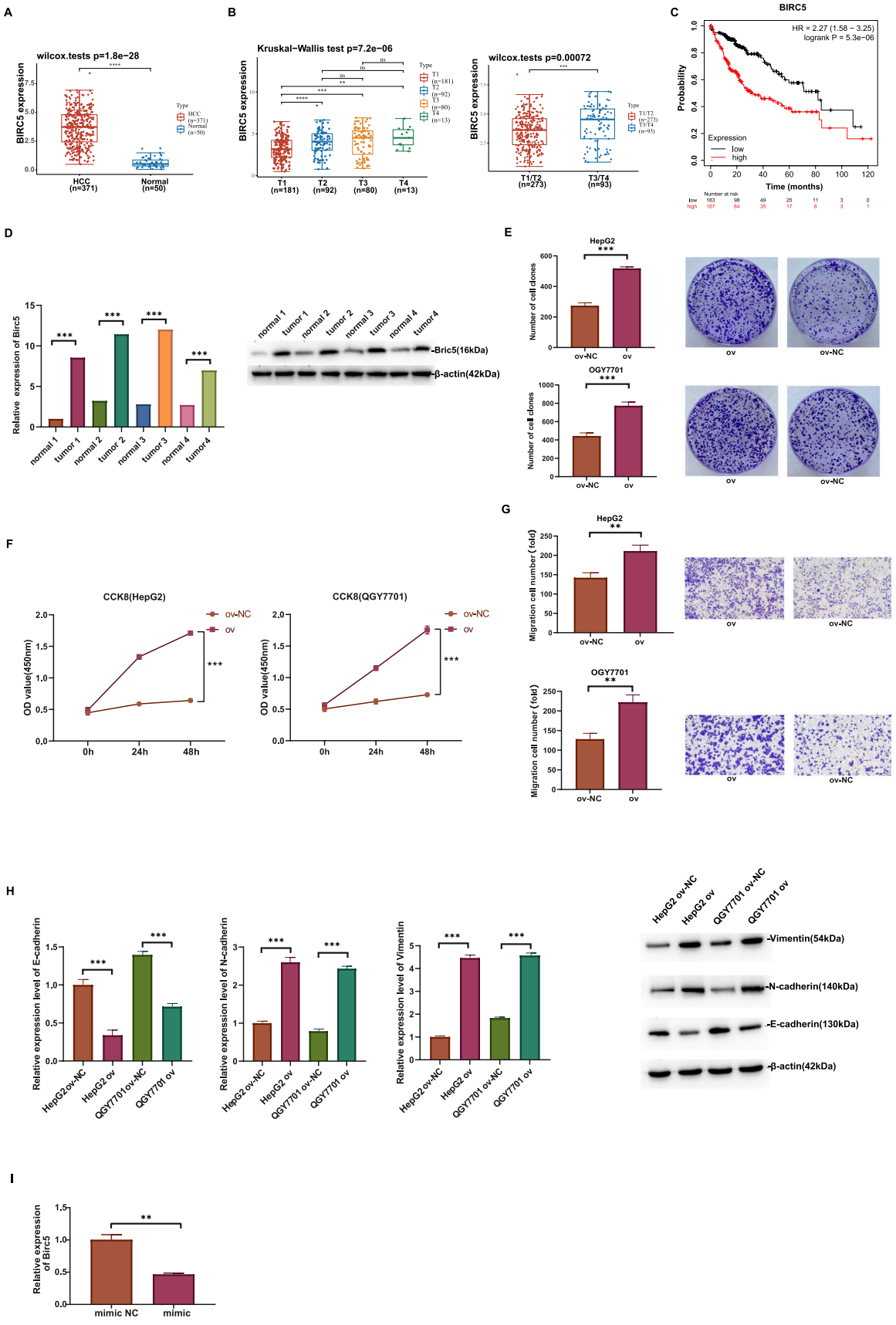
A
wilcox.tests p=1.8e−28
BIRC5 expression
HCC (n=371)
Normal (n=50)
B
Kruskal−Wallis test p=7.2e−06
T1 (n=181)
T2 (n=92)
T3 (n=80)
T4 (n=13)
wilcox.tests p=0.00072
T1/T2 (n=273)
T3/T4 (n=93)
C
BIRC5
HR = 2.27 (1.58 − 3.25)
logrank P = 5.3e−06
Probability
Expression
low
high
Time (months)
D
Relative expression of Birc5
normal 1
tumor 1
normal 2
tumor 2
normal 3
tumor 3
normal 4
tumor 4
Bric5(16kDa)
β-actin(42kDa)
E
HepG2
OGY7701
Number of cell clones
ov-NC
ov
F
CCK8(HepG2)
CCK8(QGY7701)
OD value(450nm)
0h
24h
48h
G
HepG2
OGY7701
Migration cell number (fold)
H
Relative expression level of E-cadherin
Relative expression level of N-cadherin
Relative expression level of Vimentin
HepG2 ov-NC
HepG2 ov
QGY7701 ov-NC
QGY7701 ov
Vimentin(54kDa)
N-cadherin(140kDa)
E-cadherin(130kDa)
β-actin(42kDa)
I
Relative expression of Birc5
mimic NC
mimic

◂**Fig. 2** Association between Birc5 expression and malignant behavior in HCC cells. **A** Assistant for Clinical Bioinformatics analysis revealed elevated Birc5 expression in HCC tissues. **B** Birc5 expression was significantly higher in HCC stages III and IV than in stages I and II. **C** Kaplan–Meier analysis of the association between high Birc5 expression and unfavorable prognosis in patients. **D** Protein immunoblotting experiment analyzing the Birc5 expression level in four pairs of cancer tissues and corresponding adjacent tissues, showing a significantly higher expression level in HCC tissues than in normal tissues. **E** ov-NC was the negative control group, and ov was the experimental group with Birc5 overexpression. Colony formation assay was performed in HepG2 and QGY7701 cells to compare the proliferative capacity of HCC cells between the Birc5 overexpression group and the negative control group. **F** Evaluation of HCC cell proliferation using the CCK-8 assay. **G** Transwell assay analyzing the migration and invasion capabilities of HCC cells in Birc5-overexpression and negative control groups. **H** Western blotting analysis of E-cadherin, N-cadherin, and vimentin expression levels in Birc5-overexpression and negative control groups. **I** qRT-PCR analyzing the Birc5 mRNA expression level in HCC cells in miR-101-3p overexpression and negative control groups

MiR-101-3p overexpression regulates Birc5 to inhibit the PI3K/AKT signaling pathway in HCC cells OGY7701 and HepG2

Previous studies have demonstrated that the PI3K/AKT signaling pathway can induce EMT directly or through synergistic effects with other signaling pathways [32]. Through KEGG signaling pathway enrichment analysis (Fig. 4A), we found that PI3K-Akt signaling pathway was significantly enriched in HCC related genes, and its adjusted *p* value was low, indicating that this pathway may play an important role in the occurrence and development of HCC. Therefore, we hypothesized that miR-101-3p mediates the PI3K/AKT signaling pathway by regulating Birc5. We performed Western blotting analysis to elucidate the expression trends of PI3K, p-PI3K, AKT, and p-AKT. The protein expression levels of p-PI3K and p-AKT were significantly higher in the Birc5 overexpression group than in the negative control cell group (n = 3, $p < 0.05$, Fig. 4B). Compared with the control group, miR-101-3p overexpression inhibited PI3K and AKT phosphorylation, whereas Birc5 upregulation reversed the suppression of p-PI3K and p-AKT expression (n = 3, $p < 0.05$, Fig. 4C). Therefore, miR-101-3p inhibits the PI3K/AKT signaling pathway in HCC cells by regulating Birc5 expression.

Activation of the PI3K/AKT signaling pathway promotes HCC proliferation and EMT in vivo

To further investigate the impact of PI3K/AKT signaling pathway activation on the growth of liver cancer cells, we established a subcutaneous HCC model in nude mice. Compared with the control group, tumor volume, mass, and growth rate were significantly higher in the Birc5 overexpression group (n = 5, $p < 0.05$, Fig. 5A–C). However, when the PI3K/AKT pathway inhibitor miltefosine was added, tumor volume, mass, and growth rate were reduced, suggesting that Birc5 overexpression enhances the proliferative ability of HCC cells by activating the PI3K/AKT-signaling pathway. Immunohistochemical analysis revealed significantly higher Birc5 protein expression (Fig. 5D) and Ki67 expression (Fig. 5E) in the Birc5 overexpression group than in the control group. However, when the pathway inhibitor was added, Birc5 protein and Ki67 expression levels were significantly reduced, although they remained higher than levels in the control group, indicating that Birc5 may promote tumor cell proliferation through other pathways. After addition of the PI3K/AKT pathway inhibitor (n = 4, $p < 0.05$, Fig. 5F), the N-cadherin and vimentin expression levels were reduced, whereas E-cadherin expression was increased, suggesting that Birc5 mediates the occurrence of EMT in HCC cells by activating the PI3K/AKT signaling pathway. Conversely, miR-101-3p inhibits HCC cell proliferation, invasion, and EMT by suppressing Birc5 expression.

Discussion

In recent years, advancements in medical technology, surgical techniques, and targeted drugs have substantially improved the prognosis of early-stage HCC. However, effective treatment options for advanced, metastatic HCC remain limited, resulting in a poor prognosis for affected patients. Invasion and metastasis are major contributors to the adverse prognosis of HCC. Furthermore, the molecular mechanisms underlying the invasion and metastasis of HCC are not fully understood. EMT is a crucial mechanism involved in the development of several tumors [33]. In EMT, tumor cells lose their epithelial characteristics and acquire mesenchymal features, enhancing their migration capabilities and facilitating the local infiltration, vertical invasion, and distant metastasis of tumor cells. Therefore, EMT plays a key role in initiating the malignant transformation of epithelial-derived tumors. Although the improved prognosis in early-stage HCC highlights the success of current medical interventions, challenges associated with advanced stage, metastatic disease emphasize the need for increased understanding of the molecular mechanisms involved. Investigations of the role of EMT in HCC invasion and metastasis may offer useful information concerning the development of targeted therapeutic strategies that can mitigate the progression of aggressive HCC phenotypes. Further research concerning the molecular pathways and regulatory factors governing EMT in HCC is warranted to identify potential therapeutic targets and improve patient outcomes in advanced stage disease.

MiRNAs constitute a highly conserved class of small, non-coding, single-stranded RNA molecules. Recent studies

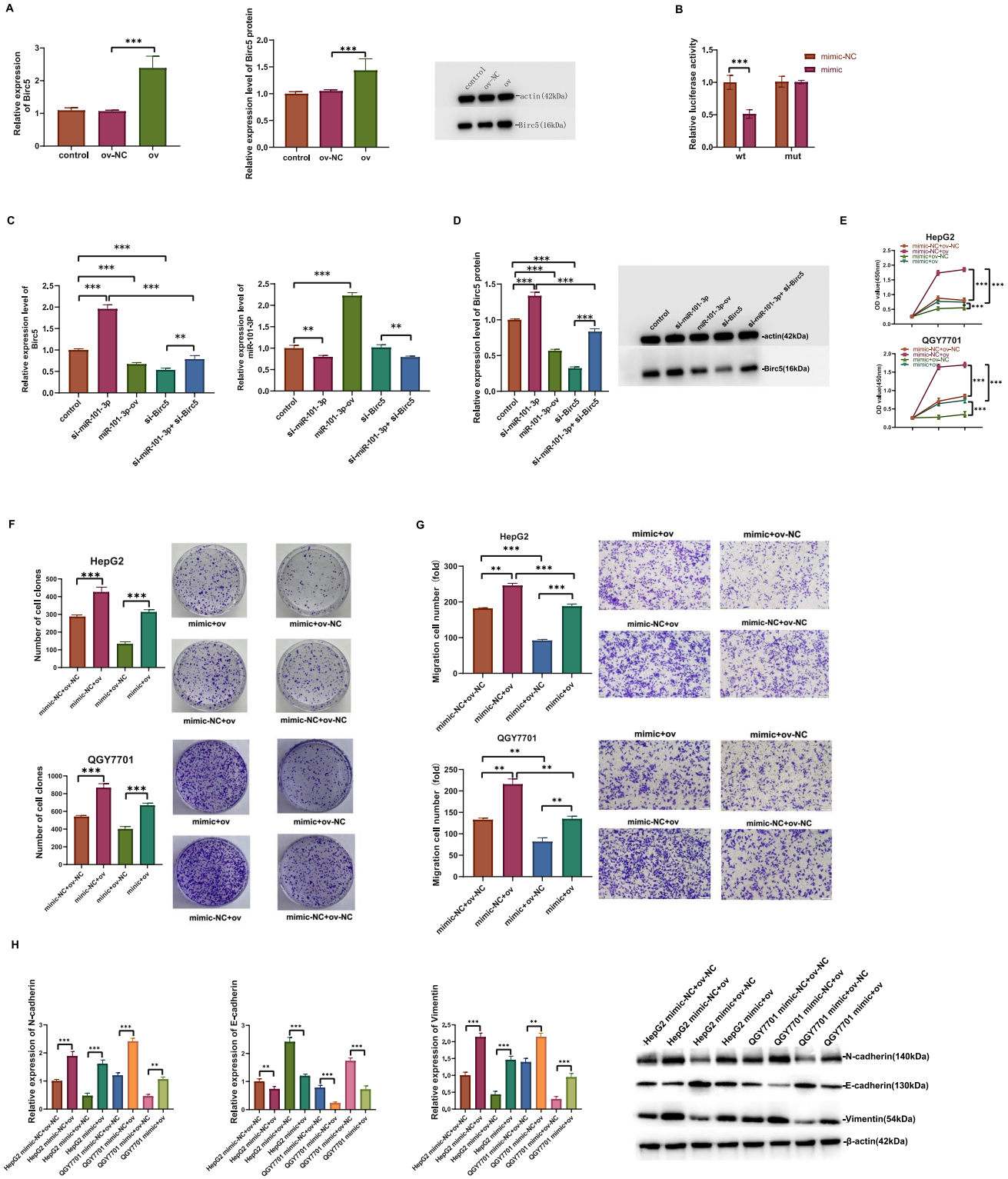

have demonstrated differential expression of miRNAs in various tumor tissues and revealed their abilities to regulate tumor cell proliferation, apoptosis, and angiogenesis, thus promoting tumor invasion and metastasis. Accordingly, miRNAs are potential therapeutic targets for cancer. A better understanding of the functions of miRNAs is crucial for the development of molecular targeted drugs. The tumor suppressor miR-101-3p is significantly downregulated in various cancer types, including breast, prostate, and head and neck cancers [34, 35]. It inhibits cancer cell proliferation,

◂**Fig. 3** Elevated Birc5 expression reverses the effects of miR-101-3p, promoting proliferation and invasion in HCC cells. **A** In the control group, negative control group, and Birc5 overexpression group, qRT-PCR and WB were performed to compare the expression levels of Birc5 in HCC cells among the three groups. **B** Luciferase assay to detect the relative luciferase activity of mRNA reporter constructs containing wild-type or mutant Birc5 3′-UTR downstream of the luciferase gene after transfection with miR-101-3p mimic or NC. **C** miR-101-3p and Birc5-specific siRNA were transfected, and the mRNA expression levels of miR-101-3p and Birc5 in each group of cells were detected by qRT-PCR. **D** miR-101-3p and Birc5-specific siRNA were transfected, and the protein expression level of Birc5 in each group was detected by Western blotting analysis. **E** In HepG2 and QGY7701 HCC cells, based on the miR-101-3p overexpression group and the control group, the expression of Birc5 was upregulated and downregulated, respectively. CCK-8 assay was performed to compare the proliferation of cells in the four groups. **F** Colony formation assay was conducted in the four groups of HCC cells to compare their proliferation capabilities. **G** Transwell assay analyzing invasive ability in HCC cells. **H** Western blot analysis was performed to compare the protein expression levels of E-cadherin, N-cadherin, and Vimentin in the four groups of HCC cells. "Mimic" refers to miR-101-3p mimic; "NC" refers to negative control

migration, and invasion. Therefore, we investigated the expression and functions of miR-101-3p in HCC, revealing that it is downregulated in HCC tissues and in the OGY7701 and HepG2 cell lines. The miR-101-3p expression level was closely associated with patient prognosis. Cell experiments demonstrated that miR-101-3p overexpression could inhibit the proliferation and invasion of OGY7701 and HepG2 cells, suggesting a tumor suppressor role for miR-101-3p in HCC cells.

Over 5,300 human genes have been identified as potential targets of miRNA [36, 37]. To understand the potential mechanisms underlying the anticancer effects of miR-101-3p in HCC, we searched for potential targets using TargetScan. The Birc5 protein is an essential member of the apoptosis protein family and has been extensively studied in recent years. Birc5 expression is closely related to the infiltration, metastasis, and proliferation of malignant tumors [38]. Birc5 regulates cellular development and the cell cycle, possessing a dual function of inhibiting apoptosis and promoting cell proliferation [39]. It is highly expressed in HCC tissues and cells, exerting a carcinogenic effect [40]. The relationship between Birc5 and EMT has also been studied in other tumors. Zhang et al. [41] found that knocking out *Birc5* in retinal pigment epithelial cells attenuated the TGF-β pathway and inhibited EMT. Zhao et al. [42] demonstrated that Birc5 induces EMT in ovarian cancer epithelial cells through the TGF-β pathway, suppressing tumor cell apoptosis. In the present study, we found that Birc5 overexpression promotes the proliferation and invasion of HCC cells. Birc5 exhibits low expression levels in normal cells but high expression levels in HCC cells. We also confirmed the role of Birc5 in EMT of HCC cells through in vitro experiments. Western blotting analysis showed that elevated Birc5 expression reduced the expression levels of epithelial cell markers, such as E-cadherin, and increased the expression levels of mesenchymal cell markers, such as N-cadherin and vimentin. E-cadherin is a crucial epithelial marker in EMT, which participates in the formation of cell adhesion structures and maintains the adhesion and integrity of epithelial cells. Reduced E-cadherin expression is associated with a loss of tight connections between cells and reduced cell adhesion, facilitating the detachment of cells from the primary tumor site and promoting increased cell motility and invasive ability. Birc5 downregulation can inhibit the EMT and proliferation of HCC cells.

The present study revealed a novel target axis (Fig. 6). Decreased miR-101-3p expression is associated with reduced inhibition of Birc5 expression, phosphorylation of the PI3K/AKT signaling pathway, enhanced proliferative and invasive capabilities of HCC cells, decreased E-cadherin expression, and increased EMT in HCC cells. When the PI3K/AKT signaling pathway was blocked, HCC cell proliferation and Birc5 expression were reduced, indicating that Birc5 induces EMT by phosphorylating the PI3K/AKT signaling pathway. In the present study, we explored the associations among miR-101-3p, Birc5, the PI3K/AKT pathway, and EMT of HCC cells. We found that miR-101-3p inhibits the activation of the PI3K-AKT signaling pathway by targeting Birc5, thereby suppressing the EMT in HCC cells. p-AKT is involved in Birc5-mediated EMT of tumors. Considering the complexity of the p-AKT signaling pathway, further studies are needed to determine whether other upstream regulatory factors are involved in Birc5-mediated enhanced p-AKT signaling. In addition to the PI3K/AKT pathway, several signaling pathways regulate EMT, including the Smad-dependent TGF-β pathway, Wnt/β-catenin pathway, and Ras-MAPK pathway [43]. These pathways exhibit overlapping phenomena. Therefore, the specific mechanism by which Birc5 regulates EMT through the PI3K/AKT pathway in HCC cells requires further exploration. Our study confirmed the presence of binding sites between miR-101-3p and Birc5; an inverse association was observed between the expression levels of Birc5 and miR-101-3p. Furthermore, miR-101-3p overexpression suppressed the tumor characteristics of HCC cells. In vivo experiments demonstrated that PI3K/AKT pathway inhibitors significantly inhibited tumor proliferation, offering a promising avenue for the development of novel HCC treatments.

Conclusion

In summary, miR-101-3p is downregulated in HCC cells and can target Birc5 to regulate the PI3K/AKT signaling pathway, thereby inhibiting the invasion, migration, EMT and proliferation of HCC cells and the development of implanted

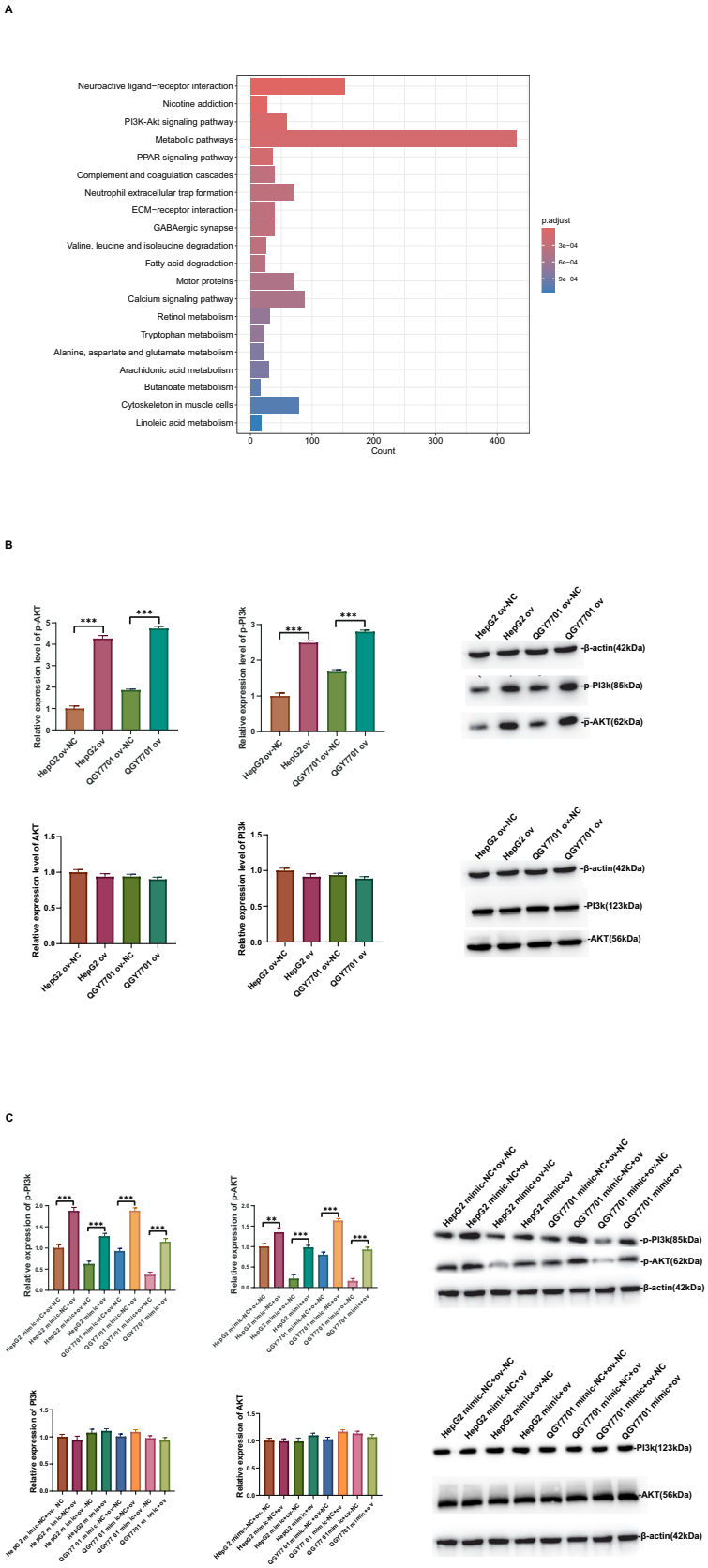

Fig. 4 miR-101-3p overexpression regulates Birc5 to inhibit the PI3K/AKT signaling pathway in HCC cells. **A** Bar plot of KEGG signaling pathway enrichment analysis. This figure shows the results of the signaling pathway enrichment analysis based on the KEGG database, which is used to evaluate the enrichment of genes related to liver cancer invasion, proliferation, and EMT in different signaling pathways. The vertical axis in the figure represents the adjusted *p*–value (p.adjust), reflecting the significance level of pathway enrichment. The smaller the *p*–value, the more significant the pathway enrichment. The horizontal axis represents the number of enriched genes (Count), reflecting the number of genes involved in each pathway. **B** Western blotting analysis of PI3K, AKT, p-PI3K and p-AKT expression levels in the Birc5 overexpression group and the control group. **C** Based on the Birc5 overexpression group and the control group, the expression of miR-101-3p was upregulated and downregulated, respectively. Western blot was used to detect the protein expression levels of PI3K, AKT, p-PI3K, and p-AKT in the four groups of cells. "p- " denotes phosphorylated forms of PI3K and AKT proteins

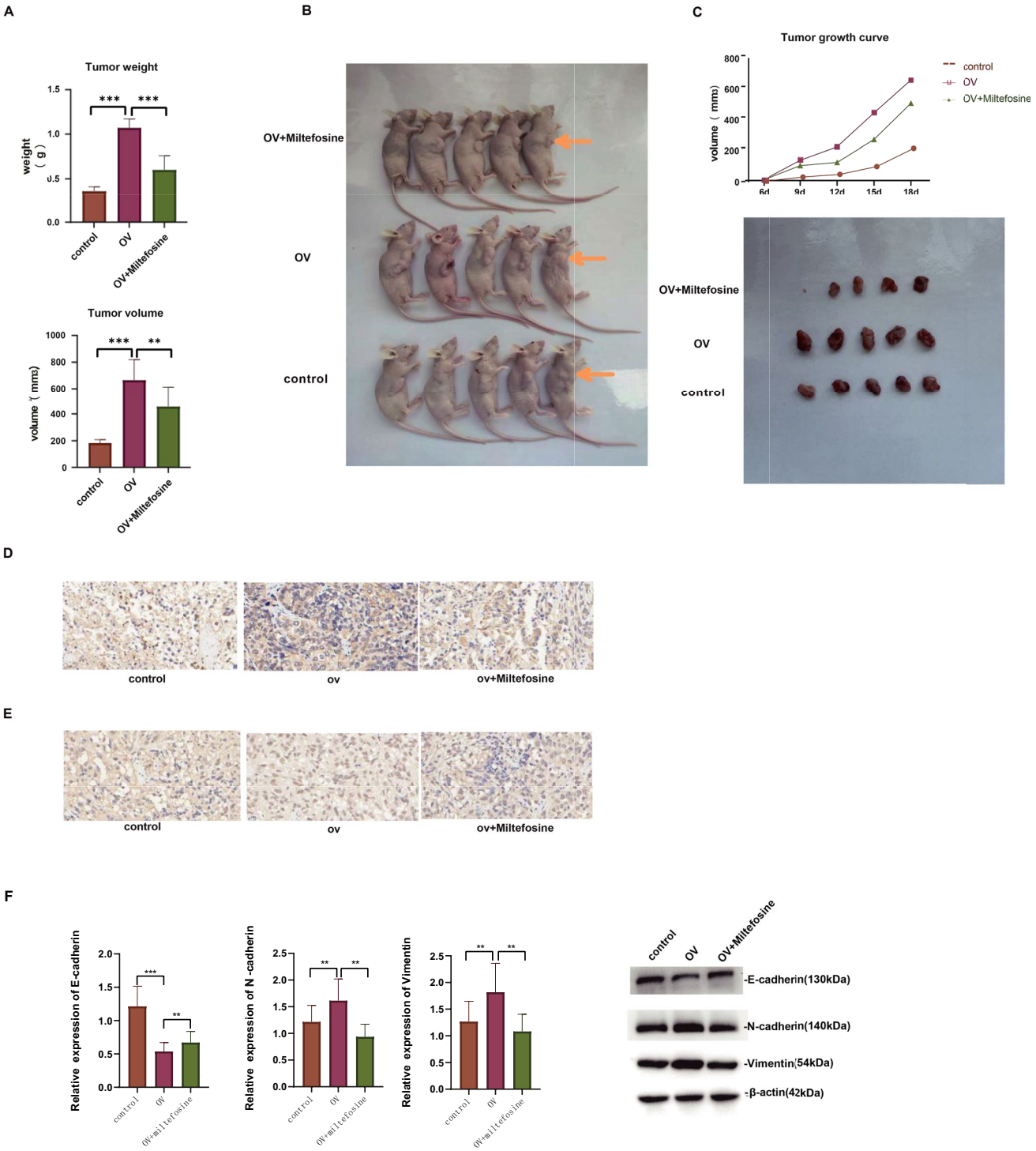

Fig. 5 Blocking the PI3K/AKT signaling pathway inhibits HCC cell proliferation and EMT. **A** Tumor cells with and without the PI3K/AKT pathway inhibitor were subcutaneously implanted in male BALB/c nude mice. Tumor mass and volume were compared among the three groups over an 18-day observation period. **B** Macroscopic appearance of tumors in nude mice after 18 days. **C** Tumor volume changes in each mouse and the tumor growth curve. Immunohistochemical assessment of **D** Birc5 expression and **E** Ki67 expression. **F** Western blotting analysis of the effects of the PI3K/AKT signaling pathway inhibitor on EMT in HCC cells

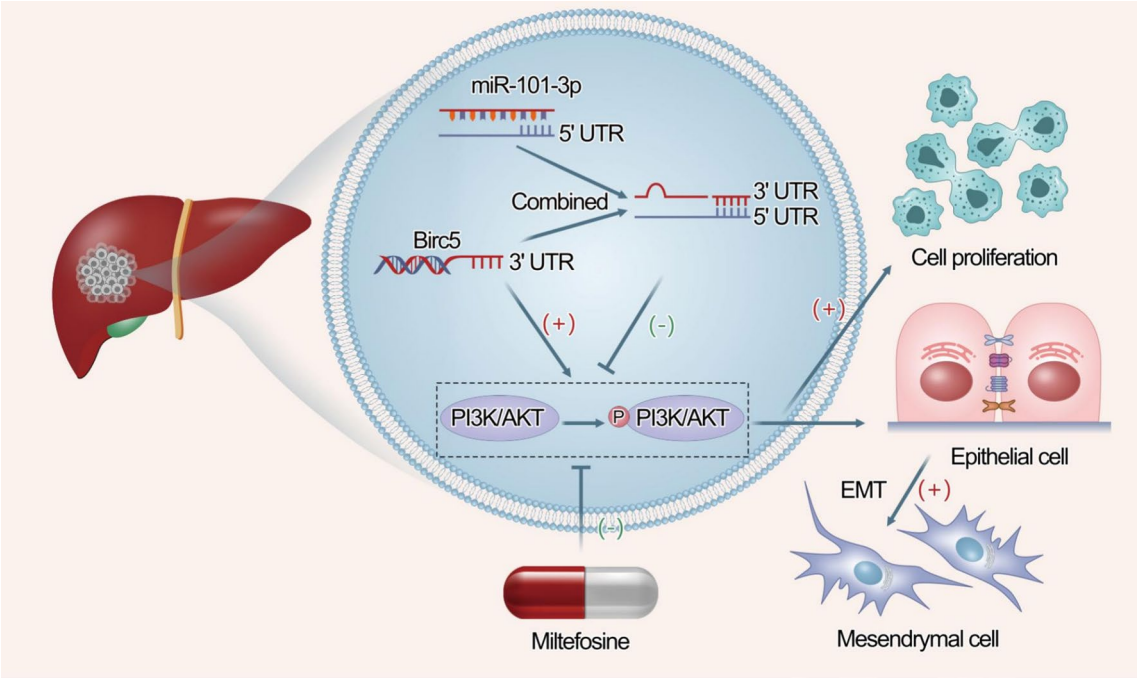

Fig. 6 Schematic representation of the function of miR-101-3p in HCC cells. In HCC cells with miR-101-3p overexpression, miR-101-3p binds to Birc5 and inhibits its expression, thereby suppressing phosphorylation of the PI3K/AKT signaling pathway and the proliferation and EMT of HCC cells

tumors in vivo. We explored the role of miR-101-3p in the development of HCC, providing a basis for targeted therapy. However, further studies are needed to determine whether miR-101-3p and Birc5 can be used as effective predictors and therapeutic targets for HCC. Overall, Birc5 is a crucial regulator of the progression and metastasis of HCC. Furthermore, miR-101-3p binds to Birc5 to mediate antitumor effects. Our results revealed mechanisms underlying the proliferation and metastasis of HCC, which can be used to develop predictive biomarkers and novel treatments in future research.

Supplementary Information The online version contains supplementary material available at https://doi.org/10.1007/s10238-025-01622-1.

Acknowledgements Not applicable.

Authors' contributions Wenyuan Zhu conducted in vitro and in vivo experiments. Zhengjian Wang and Qingqiang Ni wrote the manuscript. Wenyuan Zhu and Ruxuan Zhang completed the illustrations. Fangfeng Liu was responsible for quality control of the experiments. Hong Chang was responsible for funding acquisition and confirmed that the presentation of data/figures accurately. All authors read and approved the final manuscript.

Funding This study was supported by the Natural Science Foundation of Shandong Province, Grant/Award Number: ZR2020MH054.

Data availability The datasets generated and analyzed during the current study are available from the corresponding author upon reasonable request.

Declarations

Conflict of interests The authors of this manuscript have no conflict of interest.

Ethical approval and consent to participate The studies involving human participants were reviewed and approved by the Ethics Committee of Shandong Provincial Hospital (approval no. SWYX:NO.2022–477). All institutional and national guidelines for the care and use of laboratory animals were followed in this study.

Consent for publication Not applicable.

Open Access This article is licensed under a Creative Commons Attribution-NonCommercial-NoDerivatives 4.0 International License, which permits any non-commercial use, sharing, distribution and reproduction in any medium or format, as long as you give appropriate credit to the original author(s) and the source, provide a link to the Creative Commons licence, and indicate if you modified the licensed material. You do not have permission under this licence to share adapted material derived from this article or parts of it. The images or other third party material in this article are included in the article's Creative Commons licence, unless indicated otherwise in a credit line to the material. If material is not included in the article's Creative Commons licence and your intended use is not permitted by statutory regulation or exceeds the permitted use, you will need to obtain permission directly from the copyright holder. To view a copy of this licence, visit http://creativecommons.org/licenses/by-nc-nd/4.0/.

References

1. Ferlay J, Colombet M, Soerjomataram I, et al. Estimating the global cancer incidence and mortality in 2018: GLOBOCAN sources and methods. Int J Cancer. 2019;144(8):1941–53.
2. He J, Gu D, Wu X, et al. Major causes of death among men and women in China. N Engl J Med. 2005;353(11):1124–34.
3. Fedele M, Sgarra R, Battista S, Cerchia L, Manfioletti G. The epithelial-mesenchymal transition at the crossroads between metabolism and tumor progression. Int J Mol Sci. 2022;23(2):800.
4. Greenburg G, Hay ED. Epithelia suspended in collagen gels can lose polarity and express characteristics of migrating mesenchymal cells. J Cell Biol. 1982;95(1):333–9.
5. Onoue T, Uchida D, Begum NM, Tomizuka Y, Yoshida H, Sato M. Epithelial-mesenchymal transition induced by the stromal cell-derived factor-1/CXCR4 system in oral squamous cell carcinoma cells. Int J Oncol. 2006;29(5):1133–8.
6. Li YM, Xu SC, Li J, et al. Epithelial-mesenchymal transition markers expressed in circulating tumor cells in hepatocellular carcinoma patients with different stages of disease. Cell Death Dis. 2013;4(10): e831.
7. Kallergi G, Papadaki MA, Politaki E, Mavroudis D, Georgoulias V, Agelaki S. Epithelial to mesenchymal transition markers expressed in circulating tumour cells of early and metastatic breast cancer patients. Breast Cancer Res. 2011;13(3):R59.
8. Jiang X, Zeng L, Huang J, Zhou H, Liu Y. Arctigenin, a natural lignan compound, induces apoptotic death of hepatocellular carcinoma cells via suppression of PI3-K/Akt signaling. J Biochem Mol Toxicol. 2015;29(10):458–64.
9. Jin Y, Chen J, Feng Z, et al. The expression of Survivin and NF-κB associated with prognostically worse clinicopathologic variables in hepatocellular carcinoma. Tumour Biol. 2014;35(10):9905–10.
10. Galuppo R, Maynard E, Shah M, et al. Synergistic inhibition of HCC and liver cancer stem cell proliferation by targeting RAS/RAF/MAPK and WNT/β-catenin pathways. Anticancer Res. 2014;34(4):1709–13.
11. Inoue J, Inazawa J. Cancer-associated miRNAs and their therapeutic potential. J Hum Genet. 2021;66(9):937–45.
12. Wang J, Zeng H, Li H, et al. MicroRNA-101 inhibits growth, proliferation and migration and induces apoptosis of breast cancer cells by targeting sex-determining region Y-Box 2. Cell Physiol Biochem. 2017;43(2):717–32.
13. Guan H, Dai Z, Ma Y, Wang Z, Liu X, Wang X. MicroRNA-101 inhibits cell proliferation and induces apoptosis by targeting EYA1 in breast cancer. Int J Mol Med. 2016;37(6):1643–51.
14. Calastri M, Ferreira RF, Tenani GD, et al. Investigating VEGF. miR-145-3p, and miR-101-3p Expression in Patients with Cholangiocarcinoma. Asian Pac J Cancer Prev. 2022;23(7):2233–41.
15. Wu F, Huang W, Yang L, Xu F. MicroRNA-101–3p regulates gastric cancer cell proliferation, invasion and apoptosis by targeting PIM 1 expression. Cell Mol Biol (Noisy-le-grand). 2019;65(7):118–22.
16. Cao S, Lin L, Xia X, Wu H. lncRNA SPRY4-IT1 regulates cell proliferation and migration by sponging miR-101-3p and regulating AMPK expression in gastric cancer. Mol Ther Nucleic Acids. 2019;17:455–64.
17. Zhou H, Li L, Wang Y, Wang D. Long non-coding RNA SNHG6 promotes tumorigenesis in melanoma cells via the microRNA-101-3p/RAP2B axis. Oncol Lett. 2020;20(6):323.
18. Zhao Y, Yu Z, Ma R, et al. lncRNA-Xist/miR-101-3p/KLF6/C/EBPα axis promotes TAM polarization to regulate cancer cell proliferation and migration. Mol Ther Nucleic Acids. 2021;23:536–51.
19. Yao YL, Ma J, Wang P, et al. miR-101 acts as a tumor suppressor by targeting Kruppel-like factor 6 in glioblastoma stem cells. CNS Neurosci Ther. 2015;21(1):40–51.
20. Wang H, Guo Y, Mi N, Zhou L. miR-101-3p and miR-199b-5p promote cell apoptosis in oral cancer by targeting BICC1. Mol Cell Probes. 2020;52: 101567.
21. Zhang R, Jin S, Rao W, et al. OVA12, a novel tumor antigen, promotes cancer cell growth and inhibits 5-fluorouracil-induced apoptosis. Cancer Lett. 2015;357(1):141–51.
22. Kalliopi A, Gogas H, Polonifi K, Vaiopoulos AG, Polyzos A, Mantzourani M. Survivin beyond physiology: orchestration of multistep carcinogenesis and therapeutic potentials. Cancer Lett. 2014;347(2):175–82.
23. Salzano G, Riehle R, Navarro G, Perche F, De Rosa G, Torchilin VP. Polymeric micelles containing reversibly phospholipid-modified anti-survivin siRNA: a promising strategy to overcome drug resistance in cancer. Cancer Lett. 2014;343(2):224–31.
24. Wang J, Li Z, Lin Z, et al. 17-DMCHAG, a new geldanamycin derivative, inhibits prostate cancer cells through Hsp90 inhibition and survivin downregulation. Cancer Lett. 2015;362(1):83–96.
25. Or YY, Chow AK, Ng L, et al. Survivin depletion inhibits tumor growth and enhances chemosensitivity in hepatocellular carcinoma. Mol Med Rep. 2014;10(4):2025–30.
26. Su C. Survivin in survival of hepatocellular carcinoma. Cancer Lett. 2016;379(2):184–90.
27. Wang XJ, Chen L, Xu R, Li S, Luo GC. DLEU7-AS1 promotes renal cell cancer by silencing the miR-26a-5p/coronin-3 axis. Clin Kidney J. 2022;15(8):1542–52.
28. Han L, Lv Q, Guo K, Li L, Zhang H, Bian H. Th17 cell-derived miR-155-5p modulates interleukin-17 and suppressor of cytokines signaling 1 expression during the progression of systemic sclerosis. J Clin Lab Anal. 2022;36(6): e24489.
29. Zhang B, Liu H, Yang G, Wang Y, Wang Y. The protective effects of miR-21-mediated fibroblast growth factor 1 in rats with coronary heart disease. Biomed Res Int. 2021;2021:3621259.
30. Fäldt Beding A, Larsson P, Helou K, Einbeigi Z, Parris TZ. Pan-cancer analysis identifies BIRC5 as a prognostic biomarker. BMC Cancer. 2022;22(1):322.
31. Liu F, Sun Y, Liu B, et al. Insulin-like growth factor-1 induces epithelial-mesenchymal transition in hepatocellular carcinoma by activating survivin. Oncol Rep. 2018;40(2):952–8.
32. Wang Y, Liang Y, Yang G, et al. Tetraspanin 1 promotes epithelial-to-mesenchymal transition and metastasis of cholangiocarcinoma via PI3K/AKT signaling. J Exp Clin Cancer Res. 2018;37(1):300.
33. Luo W, Liu Q, Jiang N, Li M, Shi L. Isorhamnetin inhibited migration and invasion via suppression of Akt/ERK-mediated epithelial-to-mesenchymal transition (EMT) in A549 human non-small-cell lung cancer cells. 2019. Biosci Rep. https://doi.org/10.1042/BSR20190159.
34. Varambally S, Cao Q, Mani RS, et al. Genomic loss of microRNA-101 leads to overexpression of histone methyltransferase EZH2 in cancer. Science. 2008;322(5908):1695–9.
35. Nurul-Syakima AM, Yoke-Kqueen C, Sabariah AR, Shiran MS, Singh A, Learn-Han L. Differential microRNA expression and identification of putative miRNA targets and pathways in head and neck cancers. Int J Mol Med. 2011;28(3):327–36.
36. Lewis BP, Burge CB, Bartel DP. Conserved seed pairing, often flanked by adenosines, indicates that thousands of human genes are microRNA targets. Cell. 2005;120(1):15–20.
37. Mazière P, Enright AJ. Prediction of microRNA targets. Drug Discov Today. 2007;12(11–12):452–8.
38. Mobahat M, Narendran A, Riabowol K. Survivin as a preferential target for cancer therapy. Int J Mol Sci. 2014;15(2):2494–516.

39. Li F, Aljahdali I, Ling X. Cancer therapeutics using survivin BIRC5 as a target: what can we do after over two decades of study. J Exp Clin Cancer Res. 2019;38(1):368.
40. Liu Y, Chen X, Luo W, et al. Identification and validation of Birc5 as a novel activated cell cycle program biomarker associated with infiltration of immunosuppressive myeloid-derived suppressor cells in hepatocellular carcinoma. Cancer Med. 2023;12(15):16370–85.
41. Zhang P, Zhao G, Ji L, et al. Knockdown of survivin results in inhibition of epithelial to mesenchymal transition in retinal pigment epithelial cells by attenuating the TGFβ pathway. Biochem Biophys Res Commun. 2018;498(3):573–8.
42. Wang B, Li X, Zhao G, et al. miR-203 inhibits ovarian tumor metastasis by targeting BIRC5 and attenuating the TGFβ pathway. J Exp Clin Cancer Res. 2018;37(1):235.
43. Dongre A, Weinberg RA. New insights into the mechanisms of epithelial-mesenchymal transition and implications for cancer. Nat Rev Mol Cell Biol. 2019;20(2):69–84.

Publisher's Note Springer Nature remains neutral with regard to jurisdictional claims in published maps and institutional affiliations.